Journal of Power Sources 195 (2010) 5442–5451

Contents lists available at ScienceDirect

Journal of Power Sources

journal homepage: www.elsevier.com/locate/jpowsour

Review

Research progress in high voltage spinel $LiNi_{0.5}Mn_{1.5}O_4$ material

R. Santhanam, B. Rambabu*

Solid State Ionics and Surface Sciences Lab, Department of Physics, Southern University and A&M College, Baton Rouge, LA 70813, USA

ARTICLE INFO

Article history:
Received 25 February 2010
Received in revised form 22 March 2010
Accepted 23 March 2010
Available online 27 March 2010

Keywords:
Spinel $LiNi_{0.5}Mn_{1.5}O_4$
High voltage
Cathode material
Lithium-ion batteries

ABSTRACT

Lithium-ion batteries are now considered to be the technology of choice for future hybrid electric and full electric vehicles to address global warming. $LiCoO_2$ has been the most widely used cathode material in commercial lithium-ion batteries. Since $LiCoO_2$ has economic and environmental issues, intensive research has been directed towards the development of alternative low cost, environmentally friendly cathode materials as possible replacement of $LiCoO_2$. Among them, spinel $LiNi_{0.5}Mn_{1.5}O_4$ material is one of the promising and attractive cathode materials for next generation lithium-ion batteries because of its high voltage (4.7 V), acceptable stability, and good cycling performance. Research advances in high voltage spinel $LiNi_{0.5}Mn_{1.5}O_4$ are reviewed in this paper. Developments in synthesis, structural characterization, effect of doping, and effect of coating are presented. In addition to conventional synthesis methods, several alternative synthesis methods are also summarized. Apart from battery performance, the application of spinel $LiNi_{0.5}Mn_{1.5}O_4$ material in asymmetric supercapacitors is also discussed.

Contents

1. Introduction

Sony Corporation first introduced the concept of lithium-ion batteries in early 1990s using $LiCoO_2$ and graphite as positive and negative electrode materials, respectively. Since then, worldwide research and development have been performed enormously on lithium-ion batteries to meet increasing demand for power sources to use in portable electronic devices. Recently, energy and environmental challenges have stimulated great interest to replace gasoline engine powered vehicles by hybrid electric vehicles, plug-in hybrid vehicles and electric vehicles (HEV, PHEV and EVs). In this regard, lithium-ion batteries are attractive power source devices due to their high energy density. However, the deficiencies of current lithium-ion battery for pure EV applications are mainly energy and cost, and possibly safety. For HEV and PHEV applications, the main deficiency is cost and possibly safety and life. In this regard, many studies have been focused on the development of the cathode materials that make the energy density, power density, cycle life and safety more effective than that of $LiCoO_2$. Most of the commercial cathode materials are lithium intercalation materials with layered, spinel and olivine structures [1–4]. Fig. 1 shows the charge and discharge curves of commercially important intercalation materials studied for advanced lithium-ion batteries [5].

* Corresponding author at: Solid State Ionics and Surface Sciences Lab, Department of Physics, Southern University and A&M College, James Hall, Baton Rouge, LA 70813, USA. Tel.: +1 225 771 4130; fax: +1 225 771 2310.
E-mail address: rambabu@cox.net (B. Rambabu).

0378-7753/$ – see front matter © 2010 Elsevier B.V. All rights reserved.
doi:10.1016/j.jpowsour.2010.03.067

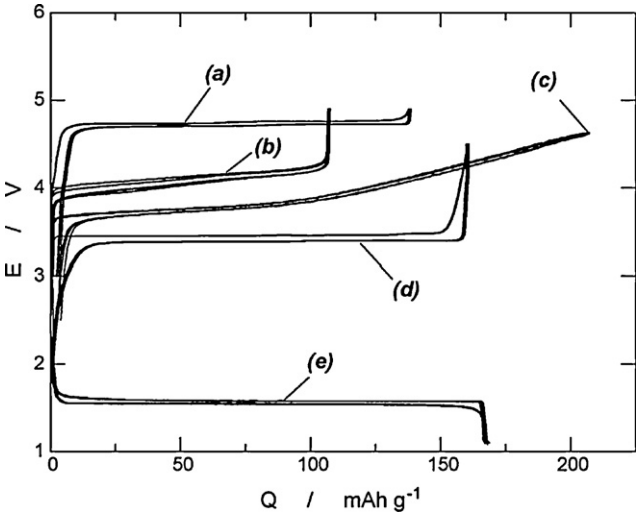

Fig. 1. Charge and discharge curves of (a) $Li[Ni_{0.5}Mn_{1.5}]O_4$, (b) $LiMn_2O_4$-based material of lithium aluminum manganese oxide (LAMO), (c) $LiCo_{1/3}Ni_{1/3}Mn_{1/3}O_2$, (d) $LiFePO_4$, and (e) $Li[Li_{1/3}Ti_{5/3}]O_4$ in nonaqueous lithium cells [5].

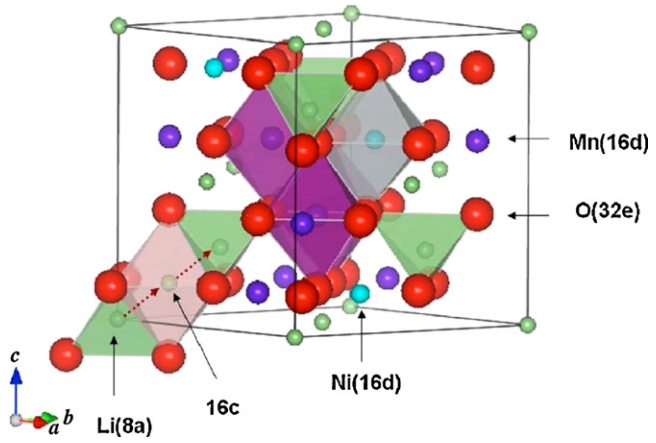

Fig. 2. The spinel structure of $LiNi_{0.5}Mn_{1.5}O_4$ (*Fd*3*m*) showing diffusion path of lithium [31].

Among the numerous transition metal oxides, manganese-based oxides are particularly attractive as cathode materials because of their low cost and non-toxicity. Among them, $LiMn_2O_4$ spinel and its derivatives have been extensively studied as promising cathode materials due to their easy preparation, abundance, low cost, and non-toxicity [6–12]. Pure $LiMn_2O_4$ has face-centered spinel structure with *Fd*3*m* space group in which the Mn, Li and O ions are in the 16d octahedral sites, 8a tetrahedral sites and 32e sites, respectively. The isotropic structure of spinel $LiMn_2O_4$ provides a 3D network for lithium-ion diffusion, and hence, this material is suitable for fast lithium insertion and deinsertion reactions [12–18]. However, it suffers from poor cycling behavior at elevated temperature [19,20]. In order to overcome this problem, many research groups have been focused on substitution of other transition metals for Mn to make $LiM_xMn_{2-x}O_4$ (M = Co, Cr, Ni, Fe, Cu, etc.) [21–25].

Sigala et al. suggested that much of the reduced capacity of Cr-doped spinel appears in 4.9 V plateau and the size of the plateau increases with Cr content [21]. Zhong et al. reported that all the metal doped spinels should be reinvestigated for the intercalation behavior in the high voltage region [26]. During the course of investigations, it has been found that a Ni-doped spinel oxide, $LiNi_{0.5}Mn_{1.5}O_4$ is the most promising and attractive one because of its good cycling behavior and relatively high capacity with one dominant plateau at around 4.7 V whereas other materials exhibited two plateaus at around 4.0 and 5.0 V [26–28]. Great attention has been given to spinel $LiNi_{0.5}Mn_{1.5}O_4$ because it provides access to redox couple (Ni^{III}/Ni^{IV}) below 4.8 V vs. Li. Since these redox couples are pinned at the top of the O–2p bands, a step between them is not observed in the spinel $LiNi_{0.5}Mn_{1.5}O_4$ [29]. $LiNi_{0.5}Mn_{1.5}O_4$ spinel is fundamentally different from pure spinels as all redox activity takes place on Ni and Mn remains in 4+ state. This spinel has two different crystal structures of the space groups of *Fd*3*m* (non-stoichiometric disordered $LiNi_{0.5}Mn_{1.5}O_{4-\delta}$) in which Mn ions are present in mainly Mn^{4+} and little Mn^{3+}, and $P4_332$ (stoichiometric ordered $LiNi_{0.5}Mn_{1.5}O_4$) in which Mn ions are only present in Mn^{4+}. The non-stoichiometric $LiNi_{0.5}Mn_{1.5}O_{4-\delta}$ has face-centered cubic spinel structure with *Fd*3*m* space group in which, like pure spinel $LiMn_2O_4$, the Ni and Mn, Li and O atoms are occupied in the 16d octahedral sites, 8a tetrahedral sites and 32e sites, respectively. In this case, Ni and Mn atoms are randomly distributed in the 16d sites. However, the stoichiometric $LiNi_{0.5}Mn_{1.5}O_4$ has primitive simple cubic structure with $P4_332$ space group in which the Ni, Mn, and Li atoms are occupied in the 4a, 12d, and 4c sites and O ions are occupied in the 8c and 24e sites [30]. In this case, Ni and Mn atoms are ordered regularly. The disordered $LiNi_{0.5}Mn_{1.5}O_{4-\delta}$ spinel was found to have better electrochemical performance than ordered spinel $LiNi_{0.5}Mn_{1.5}O_4$ [30]. Ceder and co-workers presented the diffusion path of lithium in the disordered $LiNi_{0.5}Mn_{1.5}O_{4-\delta}$ spinel as shown in Fig. 2 [31]. The theoretical capacity of $LiNi_{0.5}Mn_{1.5}O_4$ is calculated to be 147 mA h g^{-1} when all lithium-ions can be extracted from this material. The main issues with this spinel material are as follows: (i) the redox couple (Ni^{III}/Ni^{IV}) is at the potential of decomposition of the conventional battery electrolyte (1.0 M $LiPF_6$ in ethylene carbonate/diethyl carbonate) and (ii) it is difficult to prepare of pure spinel $LiNi_{0.5}Mn_{1.5}O_4$ due to the formation of $Li_xNi_{1-x}O$ as a second phase. The decomposition of electrolyte occurs at around 4.6 and 5.1 V vs. Li in half cell and full cell at room temperature, respectively. The formation of $Li_xNi_{1-x}O$ deteriorates the electrochemical performance of the spinel $LiNi_{0.5}Mn_{1.5}O_4$ material [26].

Recently, excellent reviews have been published on materials for lithium-ion batteries [4,32–34]. Chen and Cheng reported the combination of light weight elements and nanostructured materials for developing advanced lithium-ion batteries [32]. Fergus reviewed recent developments of cathode materials for lithium batteries and compared the performance of promising cathode materials and approaches for improving their performances [4]. Kim and Cho reviewed recent research advances on reversible and high capacity nanostructured electrode materials for lithium-ion batteries [33]. Synthesis procedures of $LiFePO_4$ powders, along with doped and coated derivatives, have been systematically reviewed by Jugovic and Uskokovic [34]. In the case of spinel materials, Amatucci and Tarascon reported the optimization of $LiMn_2O_4$ in their review [35] and Yi et al. [36] reviewed recent developments in the surface modifications of $LiMn_2O_4$ for lithium-ion batteries. Very recently, Nazar and co-workers published an excellent review on positive electrode materials for lithium-ion and lithium batteries [37]. They overviewed the developments of positive electrode materials in the past decade and highlighted the ultrahigh capacity systems such as Li–S and Li–air batteries for the future. Here, we tried to make a review specifically on spinel $LiNi_{0.5}Mn_{1.5}O_4$ cathode material since this material has the highest voltage (4.7 V) among all other layered cathode materials for lithium battery applications. This article provides an overview of selected developments on spinel $LiNi_{0.5}Mn_{1.5}O_4$ on synthesis, characterization, effect of doping and effect of coating on the battery performance and the application in asymmetric supercapacitors for the past decade.

2. Synthesis

2.1. Solid state method

This is the most common method in which stoichiometric mixture of starting materials is ground or ball-milled together and the resultant mixture is heat-treated in a furnace. In the case of spinel $LiNi_{0.5}Mn_{1.5}O_4$, appropriate amounts of starting materials, $NiCl_2{\cdot}xH_2O$ and $MnCl_2{\cdot}xH_2O$, are thoroughly mixed in the ratio of 1:3. Subsequently, 20% excess $(NH_4)_2C_2O_4{\cdot}H_2O$ is added to the mixture and then the mixture is ground to ensure complete reaction. After drying, the mixture is calcined at 400 °C to form the precursor containing Ni–Mn. Stoichiometric amount of Li_2Co_3 is added and mixed thoroughly. Then the mixture containing Ni–Mn–Li is calcined at different temperatures ranging from 700 to 900 °C [38]. The purity of the material depends on the starting materials, calcination temperature and time. The effect of various Ni precursors on the electrochemical performance has been investigated and the results show that the best electrochemical performance is obtained from $Ni(NO_3)_2{\cdot}6H_2O$ precursor [39]. An improved solid state reaction is reported using Li_2Co_3, NiO and electrolytic MnO_2 [40]. The morphology of the spinel $LiNi_{0.5}Mn_{1.5}O_4$ material prepared by solid state method is shown in Fig. 3a [40]. However, this method has some disadvantages such as inhomogeneity, uncontrollable particle growth and agglomeration.

2.2. Sol–gel method

The sol–gel method can overcome some disadvantages of conventional solid state method because of its low processing temperature, high chemical homogeneity, possibility of controlling size and morphology of the particles. Sol–gel method is used to prepare spinel $LiNi_{0.5}Mn_{1.5}O_4$ by various research groups [41–45]. To prepare $LiNi_{0.5}Mn_{1.5}O_4$ stoichiometric amounts of lithium acetate $[Li(CH_3COO){\cdot}2H_2O]$, manganese acetate $[Mn(CH_3COO)_2{\cdot}4H_2O]$, and nickel acetate $[Ni(CH_3COO)_2{\cdot}4H_2O]$, are dissolved in an appropriate quantity of distilled water at room temperature. The solution is stirred at 50 °C and the citric acid is added to the solution which acts as chelating agent in the polymeric matrix. The pH of the solution is adjusted to 7.0 by slowly dropping ammonium hydroxide drop wise and continued stirring for 4 h. The temperature of the solution is raised to 80–90 °C and continued stirring till the solution turned into high-viscous gel. The resulted gel is dried at 80 °C for 24 h in a temperature controlled oven of an accuracy of ±1 °C. The $LiNi_{0.5}Mn_{1.5}O_4$ precursor powder is ground to fine powder and calcined at 450 °C under oxygen flowing conditions with a constant heating followed by cooling rate at 4 °C min^{-1} to decompose organic constituents. The calcined powder is ground to a fine powder and re-sintered at different temperatures and time under oxygen flowing conditions. The morphology of the spinel $LiNi_{0.5}Mn_{1.5}O_4$ powder obtained from sol–gel method is presented in Fig. 3b [41].

2.3. Co-precipitation method

Co-precipitation procedure can easily be handled and the precipitates are generated simultaneously and uniformly dispersed throughout the solution. To synthesize $LiNi_{0.5}Mn_{1.5}O_4$ powders, the precursor $(Ni_{0.5}Mn_{1.5})(OH)_2$ is firstly prepared by dissolving stoichiometric amounts of $Ni(CH_3COO)_2{\cdot}4H_2O$, and $Mn(CH_3COO)_2{\cdot}4H_2O$ in distilled water (cationic ratio of Ni:Mn = 1:3). The aqueous solution is then precipitated by adding $NaOH/NH_4OH$ solution along with continued stirring to obtain mixed hydroxide precipitate. After filtering, washing and drying in a vacuum oven at 50–60 °C overnight, the obtained precursor is mixed with required amount of LiOH and calcined at various temperatures to get $LiNi_{0.5}Mn_{1.5}O_4$ powders. This powder is prepared by co-precipitation using different precursors such as metal sulfate, metal carbonate, and metal chlorides [46–48]. A representative image of the $LiNi_{0.5}Mn_{1.5}O_4$ material prepared by co-precipitation is shown in Fig. 3c [46].

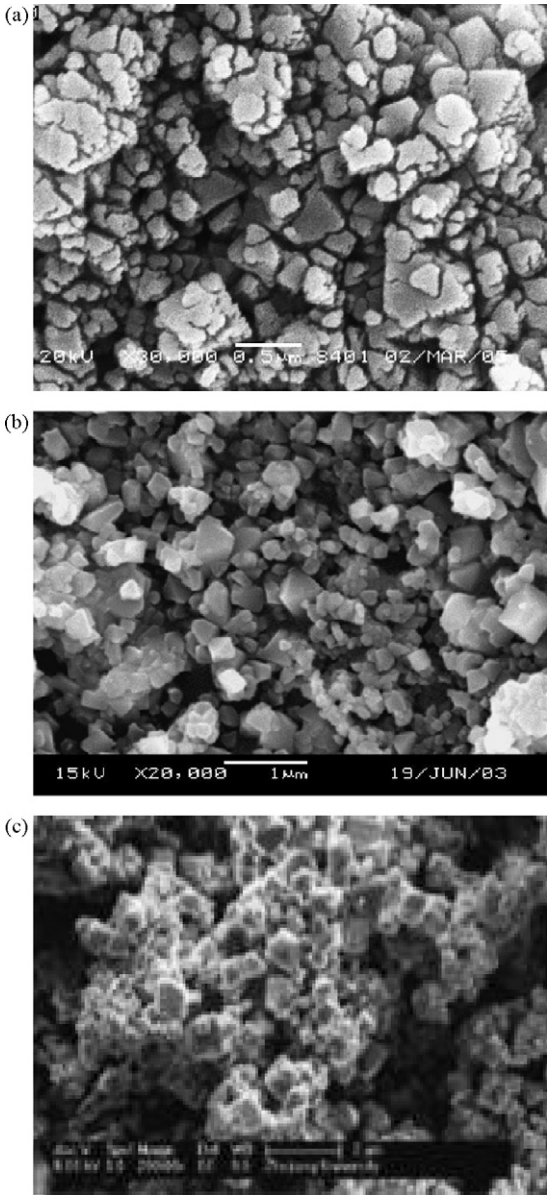

Fig. 3. SEM images of the spinel $LiNi_{0.5}Mn_{1.5}O_4$ synthesized by (a) solid state, (b) sol–gel, and (c) co-precipitation methods [40,41,46].

2.4. Other methods

High rate capability was achieved by the nano-rod like $LiNi_{0.5}Mn_{1.5}O_4$ spinel powder prepared by polymer assisted (PA) synthesis in which polyethylene glycol (PEG 400) was used as sacrificial template [49]. Homogeneous mixing of starting materials at the atomic scale was achieved by radiated polymer gel (RPG) method in which the solution containing starting materials and acrylic acid to synthesize $LiNi_{0.5}Mn_{1.5}O_4$ spinel. The solution is polymerized under the condition of Co60 γ-ray irradiation (intensity 55–75 Gy min^{-1}) [50]. 50 nm sized $LiNi_{0.5}Mn_{1.5}O_4$ having the *Fd*3*m* cubic spinel structure is readily prepared by the emulsion drying (ED) method which can intermix cations (Li, Mn and Ni) on

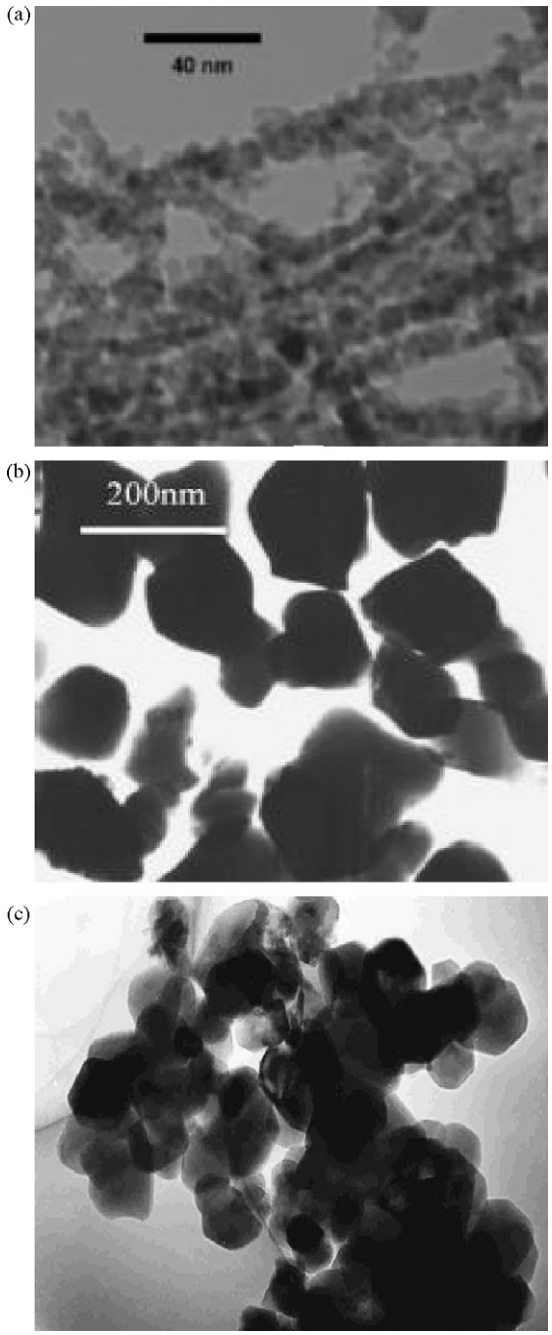

Fig. 4. TEM images of the spinel $LiNi_{0.5}Mn_{1.5}O_4$ synthesized by (a) polymer assisted, (b) radiated polymer gel, and (c) emulsion drying methods [49–51].

the atomic scale [51]. The TEM images of $LiNi_{0.5}Mn_{1.5}O_4$ material prepared by PA, RPG and ED methods are shown in Fig. 4a–c, respectively [49–51]. Oh et al. employed mechanochemical process, to synthesize $LiNi_{0.5}Mn_{1.5}O_4$ material, in which planetary-type ball mill was adopted for the mechanical activation of the starting materials [52]. This method is a common method which uses high energy ball milling to prepare highly homogeneous powders of different species by mechanical activation. The frictional energy formed by the balls and powders and rotation of the bowl would initiate some reactions between the raw materials [53,54]. The morphology of the material prepared by mechanochemical method is shown in Fig. 5a [52]. Fang et al. reported a combinational annealing method to prepare the spinel $LiNi_{0.5}Mn_{1.5}O_4$ material [55]. Since high temperature calcination results in oxygen loss, Ni defi-

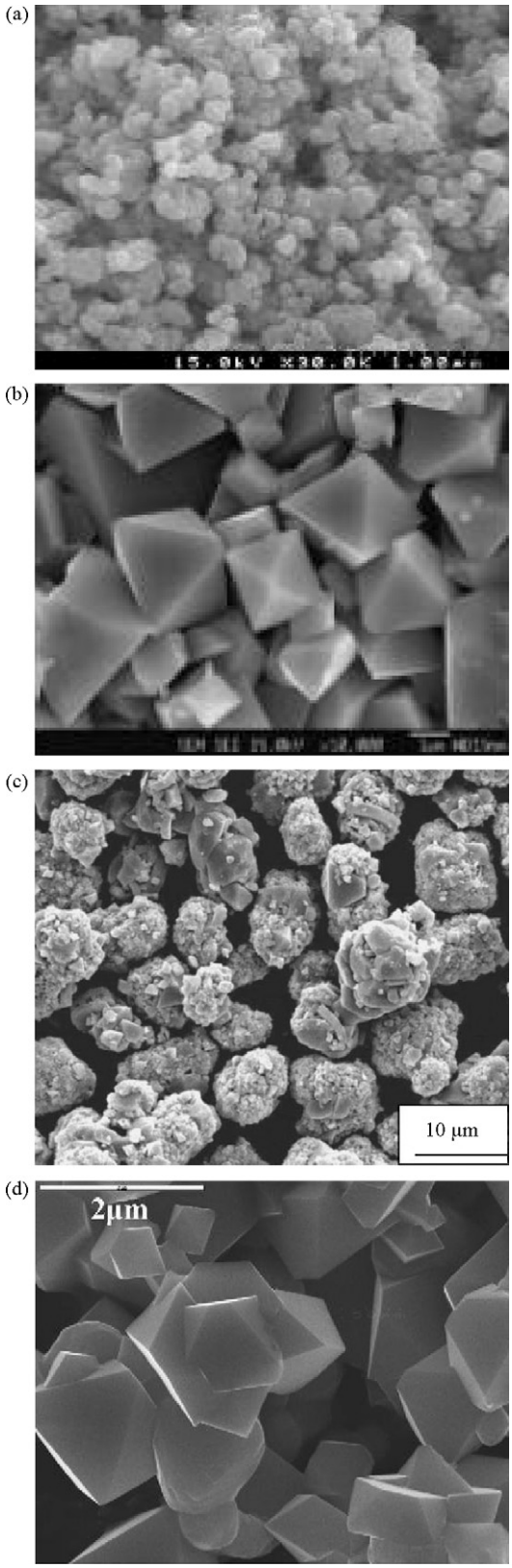

Fig. 5. SEM images of the spinel $LiNi_{0.5}Mn_{1.5}O_4$ synthesized by (a) mechanochemical, (b) and (c) molten salt, and (d) carbon combustion methods [52,61,62,65].

ciency and formation of impurity phases, the cycling performance of the material would be deteriorated. Oxygen loss can be recovered by low rate cooling or low temperature annealing [56,57]. Therefore, in the combinational annealing method, the mixed precursors were heated to high temperature and then quickly cooled down to low temperature for isothermal annealing treatment. In this way, $LiNi_{0.5}Mn_{1.5}O_4$ material can be prepared with minimum oxygen loss, reduced impurity to obtain good electrochemical performance.

The main disadvantages of wet methods are high cost and complicated synthetic procedure. Molten salt (MS) method is a simple technique to prepare complex oxide materials. This method is based on the use of a salt with low melting point such as alkali metal sulfates, hydroxides, carbonates and chlorides. Highly pure materials can be prepared at relatively low temperatures in MS method due to relatively higher diffusion rates between reaction components. Various lithium salts are used to prepare lithium manganese oxides and lithium cobalt oxide using MS method [58–60]. Spherical and well-ordered highly crystalline $LiNi_{0.5}Mn_{1.5}O_4$ materials are prepared by MS method by different research groups [61,62]. The SEM images of highly crystalline and spherical $LiNi_{0.5}Mn_{1.5}O_4$ materials prepared by MS method are shown in Fig. 5b and c [61,62]. Combustion reaction method is also used for the preparation of various oxide materials [63,64]. Zhang et al. used carbon combustion method (CCS) to prepare cubic $LiNi_{0.5}Mn_{1.5}O_4$ material with a space group of *Fd*3*m* using carbon as fuel [65]. In this CCS method, the structure and particle size could be adjusted by the amount of carbon used for combustion. A representative SEM image of the $LiNi_{0.5}Mn_{1.5}O_4$ material prepared by CCS method is shown in Fig. 5d [65].

3. Characterization

It is known that the synthesis of pure phase of $LiNi_{0.5}Mn_{1.5}O_4$ is somewhat difficult due to the presence of unwanted impurities such as NiO and Li_xNi_yO. As mentioned earlier, Sun and co-workers successfully synthesized the ordered and disordered spinels by molten salt method [30]. To prepare the disordered spinel, the precursors were mixed and calcined at 900 °C for 3 h in a covered alumina crucible. The disordered spinel powders thus obtained were oxidized to ordered spinel by heating at 700 °C for 48 h in air. The ordered ($LiNi_{0.5}Mn_{1.5}O_4$) and disordered ($LiNi_{0.5}Mn_{1.5}O_{4-\delta}$) forms of the spinel material could be differentiated by X-ray diffraction (XRD) measurements. Rietveld analysis was performed on the XRD patterns to identify the ordered and disordered structures of the spinel material. Rietveld refinement profiles are shown in Fig. 6 [30]. Small peaks representing superstructure were observed for ordered spinel but these peaks were absent in the case of disordered spinel. Similar results were also observed for other spinels such as $LiMg_{0\cdot5}Mn_{1.5}O_4$ and $LiZn_{0.5}Ti_{1.5}O_4$ [66,67]. Recently, Shaju and Bruce synthesized nanosized ordered and disordered forms of the spinel using resorcinol–formaldehyde route [68]. These authors used lattice parameters obtained from XRD analysis to differentiate the two forms of the spinel material. In the ordered spinel, the oxidation states of Ni and Mn are +2 and +4, respectively, whereas a small amount of oxygen loss in the disordered spinel is compensated by the formation of Mn^{3+}. Since the size of Mn^{3+} is bigger than Mn^{2+}, the cubic lattice parameter is larger in disordered (8.1733 Å) than that of ordered spinel (8.1677 Å). Interestingly, transmission electron microscopy (TEM) was used to observe the structural differences between ordered $LiNi_{0.5}Mn_{1.5}O_4$ and disordered $LiNi_{0.5}Mn_{1.5}O_{4-\delta}$ spinels and the results are shown in Fig. 7 [30]. The disordered spinel showed electron diffraction pattern of a typical spinel and however, the ordered spinel showed extra diffraction spots (superlattice pattern) in addition to the spots observed for pure spinel.

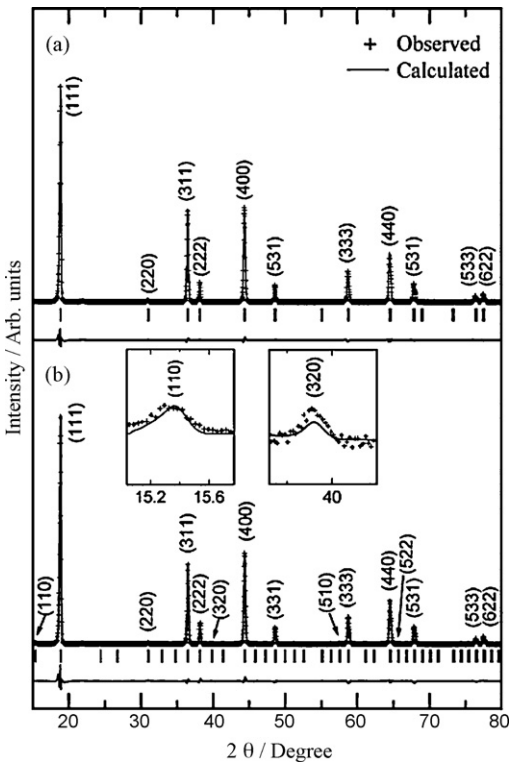

Fig. 6. Rietveld refinement profiles of XRD data for (a) $LiNi_{0.5}Mn_{1.5}O_{4-\delta}$, and (b) $LiNi_{0.5}Mn_{1.5}O_4$ powders [30].

Cyclic voltammetry is an excellent electrochemical technique to study the redox reactions and it has been widely used by electrochemists in various research fields. This technique was conveniently used to characterize the spinel $LiNi_{0.5}Mn_{1.5}O_4$ material by different research groups [31,41,46]. A typical cyclic voltammogram of disordered spinel $LiNi_{0.5}Mn_{1.5}O_{4-\delta}$ is shown in Fig. 8 [31]. Three well-defined reversible peaks were observed during charge and discharge. The appearance of 4 V peak was due to Mn^{3+} ions which were formed by the oxygen loss during high temperature calcinations. The two major peaks appearing between 4.5 and 5 V during charge and discharge cycling were due to the redox couples Ni^{2+}/Ni^{3+} and Ni^{3+}/Ni^{4+} or ordering of lithium and vacancies at $x = 0.5$ [69,70]. For ordered spinel, the 4 V peaks were absent because oxidation states of Ni and Mn were +2 and +4, respectively [30]. Charge and discharge measurements were used to characterize and differentiate ordered and disordered spinel $LiNi_{0.5}Mn_{1.5}O_{4-\delta}$ materials. The first two cycles of charge and discharge voltage profiles of two different spinels are shown in Fig. 9 [68]. The difference in charge capacity between first and second cycle was due to electrolyte oxidation [71,72]. The voltage step appearing around 4.7 V was more clear in the case of disordered spinel [71–73]. This difference in the voltage plateau could be used to identify if the spinel material was ordered or disordered. A small step appearing around 4 V in the disordered material was associated with the $Mn^{3+/4+}$ redox couple [71–73].

4. Effect of doping

Many different elements can be doped into the high voltage $LiNi_{0.5}Mn_{1.5}O_4$ spinel structure, and they impact the structure, its stability on lithium insertion/deinsertion, and the capacity retention on cycling. The use of high voltage material may have adverse effects such as possible electrolyte decomposition which may increase capacity fading on cycling. To improve the high voltage electrochemical performance of $LiNi_{0.5}Mn_{1.5}O_4$ spinel, various

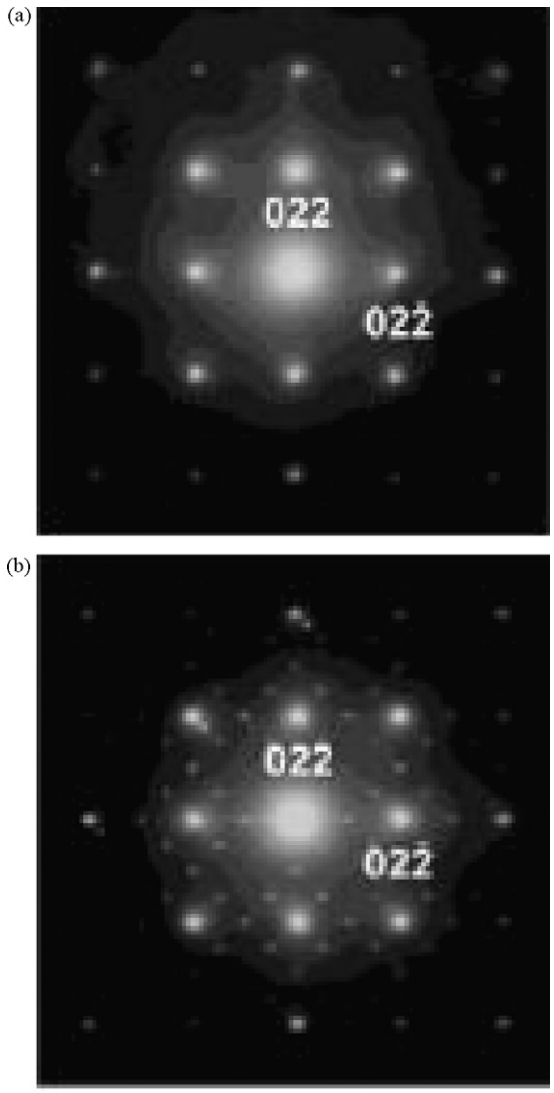

Fig. 7. Electron diffraction patterns of (a) $LiNi_{0.5}Mn_{1.5}O_{4-\delta}$ and (b) $LiNi_{0.5}Mn_{1.5}O_4$ phases in the [99] zone [30].

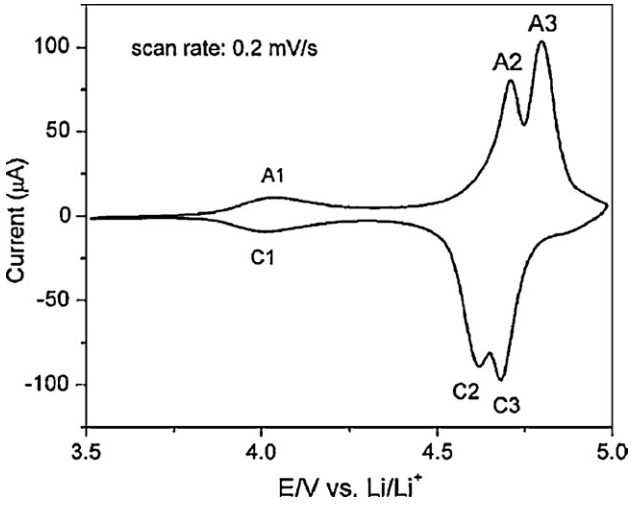

Fig. 8. Cyclic voltammogram of $LiNi_{0.5}Mn_{1.5}O_4$ electrode cycled between 3.5 and 5 V vs. Li/Li^+ at 0.2 mV s^{-1} scan rate [30].

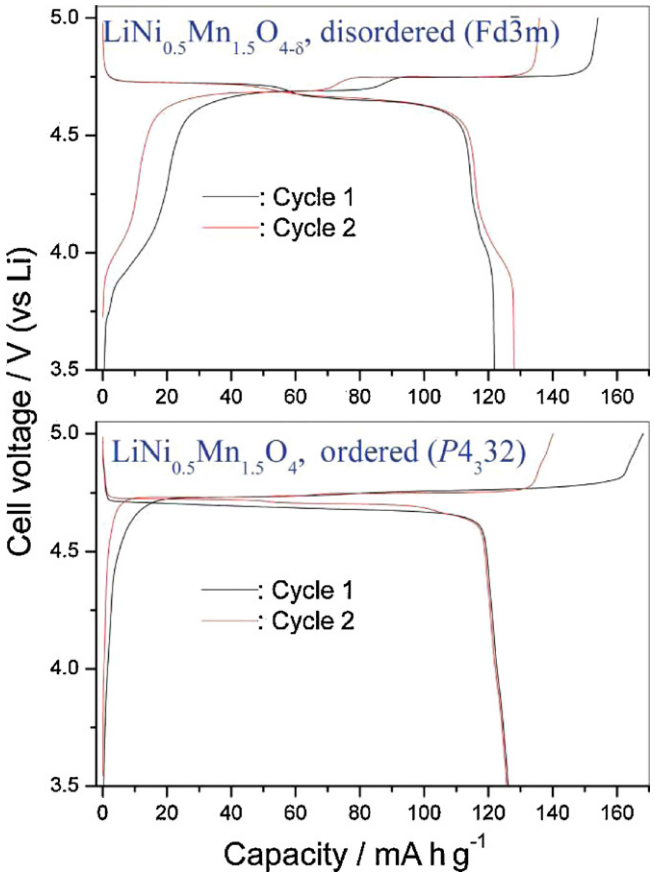

Fig. 9. Charge and discharge voltage profiles for the first and second cycles at 30 °C and 75 mA h g^{-1} between 3.5 and 5.0 V for (a) the disordered phase and (b) the ordered phase [68].

dopants have been proposed by different research groups. Titanium (Ti) was added as a dopant in the $LiNi_{0.5}Mn_{1.5}O_4$ spinel structure [74,75]. Ti doping improved the disordering of the transition metals and consequently lowers the symmetry from primitive simple cubic structure ($P4_332$) to face-centered spinel ($Fd3m$). In addition, the Ti doped $LiNi_{0.5}Mn_{1.5-x}Ti_xO_4$ spinel exhibited higher operating voltage, faster lithium diffusion and better rate capability than undoped spinel. However, the capacity was decreased on doping of larger amount of Ti due to blocking of migration pathway of electrons in octahedral sites. Voltage profiles of $LiNi_{0.5}Mn_{1.5-x}Ti_xO_4$ spinel with various amounts of Ti doping are shown in Fig. 10 [74]. Alcantara et al. also reported that the doping of small amounts of Ti improved the electrochemical performance whereas a deterioration of the reversible capacity was observed for large amounts of Ti [75]. Iron (Fe) was used as a dopant for $LiNi_{0.5}Mn_{1.5}O_4$ spinel and it was shown to improve the electrochemical performance [76,77]. The presence of Fe in the tetrahedral sites of the structure stabilizes the solid during extended cycling. The electrochemical performance of $LiNi_{0.5}Mn_{1.5}O_4$ spinel was also studied by double substitution with Ti and Fe [78]. The material containing 0.05Fe + 0.05Ti showed a two phase mechanism of lithium extraction and in contrast, the material containing 0.10Fe + 0.10Ti showed only one phase. It was suggested that the best capacity retention could be achieved by using the $LiFe_{0.10}Ti_{0.10}Ni_{0.45}Mn_{1.35}O_4$ composition associated with single phase mechanism combined with structural stabilization by Ti.

Chromium (Cr) could be added to the $LiNi_{0.5}Mn_{1.5}O_4$ spinel structure as a dopant [79–81]. The influence of Cr content on the electrochemical performance of the spinel was studied in detail. It was reported that the particle size depended on Cr content.

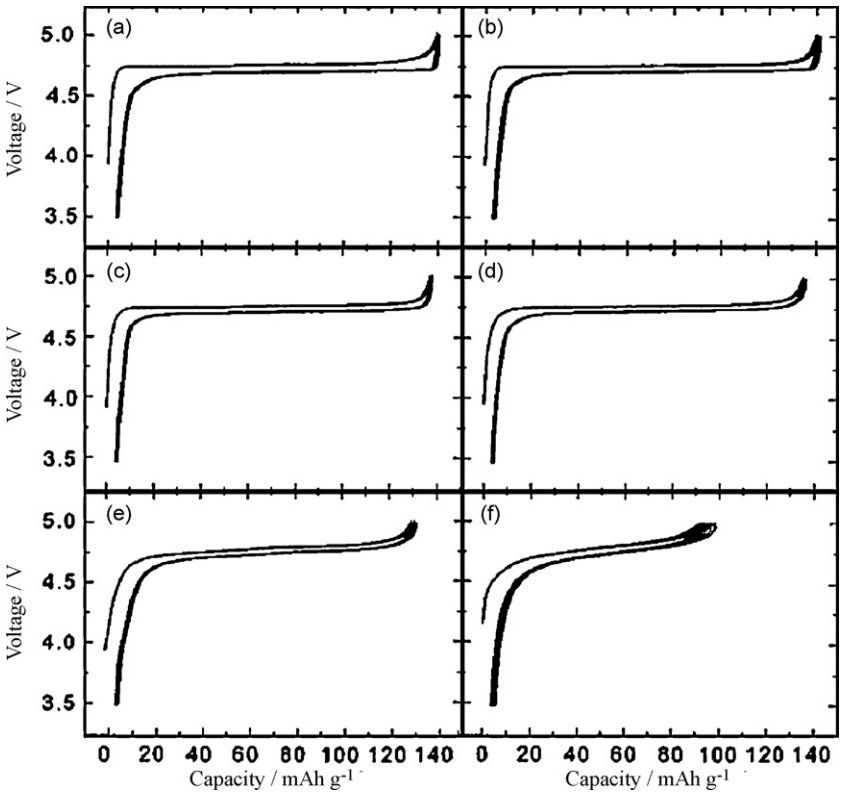

Fig. 10. Voltage profiles of $LiNi_{0.5}Mn_{1.5-x}Ti_xO_4$ with various amounts (x) of Ti doping: (a) $x = 0$, (b) $x = 0.05$, (c) $x = 0.1$, (d) $x = 0.2$, (e) $x = 0.3$, and (f) $x = 0.5$ [74].

Moreover, Cr-doped spinel delivered higher discharge capacity and capacity retention than that of undoped spinel. Another element that was used as a dopant for $LiNi_{0.5}Mn_{1.5}O_4$ spinel was ruthenium (Ru) [82]. The rate capability and cycling performance were significantly improved by Ru doping. High capacity of the Ru doped spinel was due to minimized polarization and improved electrical conductivity. The enhanced rate capability and cyclability resulted from improved structural stability of $LiNi_{0.5}Mn_{1.5}O_4$ spinel by Ru. Zirconium (Zr) and aluminum (Al) also have similar effects like other dopants. From Raman spectra, Oh et al. found that the structure of the Al and Zr doped materials was ordered spinel and Cr doped spinel was disordered. They believed that the excellent electrochemical properties of the Cr-doped spinel might be due to high electrical conductivity, chemical and structural stability [83]. Magnesium (Mg) doping was shown to improve the performances of $LiNi_{0.5}Mn_{1.5}O_4$ spinel [84]. $LiMg_{0.07}Ni_{0.43}Mn_{1.5}O_4$ material was prepared by solid state, sol–gel and xerogel methods and the electrochemical performances were compared. It was found that the spinel materials prepared by sol–gel and xerogel methods were better than solid state method. This was due to sub-micron sized particles of single crystals together with nanoparticles obtained from sol–gel and xerogel methods.

Another dopant that could be occupied in the anion site is fluorine which was a common dopant in the field of lithium-ion batteries. The reversible capacity of high voltage $LiNi_{0.5}Mn_{1.5}O_4$ spinel material was improved by fluorine doping ($LiNi_{0.5}Mn_{1.5}O_{3.975}F_{0.05}$) [85]. It was reported that the performance improvement was mainly because of suppression of the formation of NiO impurity during synthesis. Fluorine doping in the oxygen sites of the spinel could change the lattice parameters and bonding energy as reported by Du et al. [86]. They prepared the spinel material with different fluoring contents. For the materials with fluorine beyond 0.1 instead of oxygen, the capacity decreased but the cyclability was significantly improved. This result was due to fine-structure arising from fluorine doping.

5. Effect of coating

It should be noted that lithium transition metal oxides can react with the electrolyte and lead to safety issues. Significant efforts have made by different research groups to increase the stability of lithium metal oxides. It was shown that better stability can be achieved by coating the materials with stabilizing surface layer. Lithium metal oxides were coated with various oxides and phosphates and demonstrated improved capacity retention during cycling. Surface modifications of $LiNi_{0.5}Mn_{1.5}O_4$ spinel material by coating various oxides and phosphates such as ZnO [87–90], SnO_2 [91], Li_3PO_4 [92], and different metal treatments such as Zn [93], Au [94], Ag [95] have been widely investigated. In the case of ZnO-coated $LiNi_{0.5}Mn_{1.5}O_4$, the ZnO-coated electrode delivered the capacity of 137 mA h g^{-1} without any capacity loss even after 50 cycles at 55 °C as shown in Fig. 11 [88]. $LiNi_{0.5}Mn_{1.5}O_4$ surface was protected by ZnO coating, suppressed Mn dissolution and increased the structural stability. ZnO played an important role in reducing the HF content in the electrolyte. The ZnO coating layer was acted like a scavenger of fluoride anions from HF generated from the decomposition of $LiPF_6$ salt in the electrolyte by transforming HF to ZnF_2 [87–90]. Similarly, SnO_2 coating on the surface of the $LiNi_{0.5}Mn_{1.5}O_4$ improved capacity retention and the improvement enhanced with increased SnO_2 content. Based on the X-ray photoelectron spectroscopy results, Fan et al. showed that the main reason for the electrochemical stability was due to relatively low content of LiF in the SnO_2 coated $LiNi_{0.5}Mn_{1.5}O_4$ [91]. In a similar manner, Li_3PO_4 coating protects the surface of the $LiNi_{0.5}Mn_{1.5}O_4$ material and function as a solid electrolyte interface between $LiNi_{0.5}Mn_{1.5}O_4$ and solid polymer electrolyte (SPE) to pre-

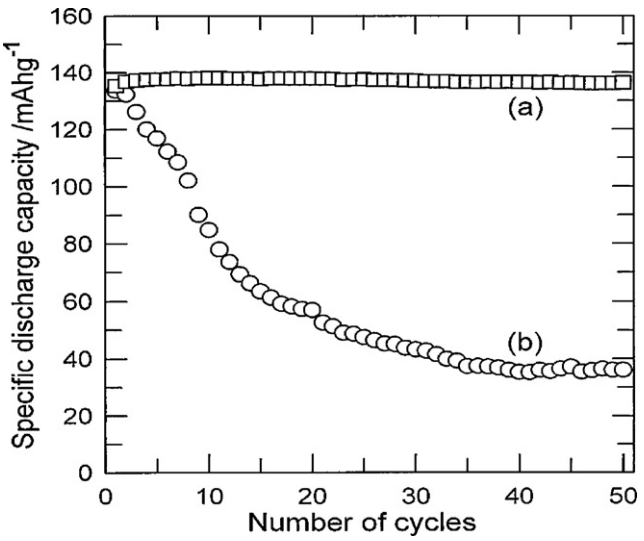

Fig. 11. Specific discharge capacity of (a) the as-prepared $LiNi_{0.5}Mn_{1.5}O_4$ and (b) ZnO-coated $LiNi_{0.5}Mn_{1.5}O_4$ electrodes at 55 °C at constant current densities of 0.4 mA cm^{-2} [88].

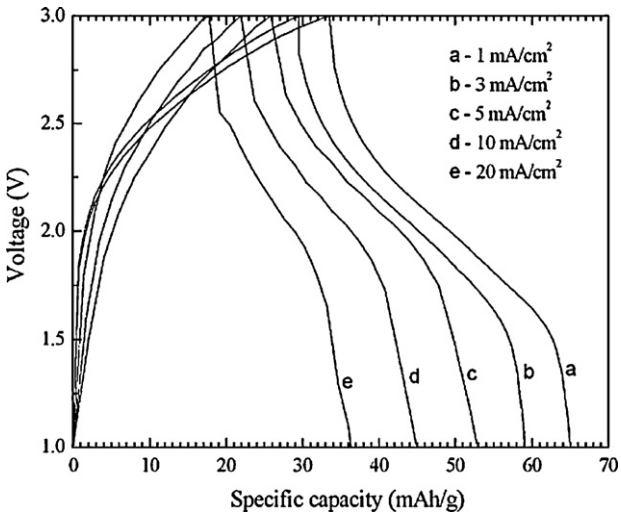

Fig. 12. Charge/discharge curves of the $LiNi_{0.5}Mn_{1.5}O_4$/AC hybrid supercapacitor at different discharge current densities in 1M$LiPF_6$ in EC/DMC electrolyte between 1.0 and 3.0 V [109].

vent the degradation of SPE [92]. Metals such Zn, Au and Ag were also coated on spinel $LiNi_{0.5}Mn_{1.5}O_4$ material and improvements in the electrochemical performance were demonstrated [93–95]. Arrebola et al. studied the effect of Au coating on the performance of $LiNi_{0.5}Mn_{1.5}O_4$ and the coating had a beneficial effect and it significantly increased the capacity. The role of the Au was to hinder the unwanted reactions and simultaneously prevent the active material particles from reacting with decomposition products such HF which was the main reason for Mn dissolution [94]. The same authors studied the adverse effect of Ag treatment on the electrochemical performance of $LiNi_{0.5}Mn_{1.5}O_4$. Ag treatment had only limited benefit at low current densities and at moderate and high current densities the capacity delivered was relatively low for Ag-treated spinel than that of untreated spinel [95]. Recently, Kang et al. coated the spinel $LiNi_{0.5}Mn_{1.5}O_4$ with BiOF and studied the electrochemical performance [96]. Spinel $LiNi_{0.5}Mn_{1.5}O_4$ powders were coated with BiOF to improve their electrochemical performances. The BiOF-coated $LiNi_{0.5}Mn_{1.5}O_4$ showed significantly improved capacity retention than that of the uncoated one. The rate capability of the BiOF-coated $LiNi_{0.5}Mn_{1.5}O_4$ was also significantly enhanced. It was suggested that the improved electrochemical performance was attributed to the scavenging HF by BiOF layer from the electrolyte. Very recently, Amine's group has reported a remarkable improvement in cycling stability at 55 °C by coating the spinel $LiNi_{0.5}Mn_{1.5}O_4$ particles with ZrO_2. The ZrO_2 coating also improved the thermal stability of $LiNi_{0.5}Mn_{1.5}O_4$ cathode due to the suppression of interfacial resistance between cathode and electrolyte by protecting the electrolyte reactivity with cathode surface [97].

6. Cathode for asymmetric supercapacitors

Electrochemical supercapacitors are attractive and new energy storage devices due to their high power density, long cycle life, low self-discharge and high safety [98]. Electrochemical capacitors are divided as electrochemical double layer capacitor and redox capacitor depending on the electrode materials used and the charge storage mechanism [99–101]. Recently, asymmetric supercapacitors have received considerable attention because they offer advantages of both supercapacitors and batteries [102,103]. This type of electrochemical system combines faradaic battery electrode and a double layer capacitor electrode [104]. Various battery materials including $LiMn_2O_4$, $LiCoO_2$ and $LiNi_{1/3}Co_{1/3}Mn_{1/3}O_2$ were used as electrode materials in asymmetric supercapacitors [105–108]. Recently, Zhao et al. studied the pseudocapacitance properties of activated carbon/$LiNi_{1/3}Co_{1/3}Mn_{1/3}O_2$ asymmetric supercapacitor in aqueous electrolyte [109]. This system exhibited an excellent cycling performance. Among the various battery cathode materials, spinel $LiNi_{0.5}Mn_{1.5}O_4$ material was a promising 5 V cathode material. The possibility of using this high voltage intercalation material as the positive electrode in combination with activated carbon negative electrode to fabricate an asymmetric supercapacitor was exploited by Rambabu and co-workers [110] and Li et al. [111]. The charge and discharge curves of the $LiNi_{0.5}Mn_{1.5}O_4$/AC hybrid supercapacitor at different current densities are presented in Fig. 12. This system exhibited excellent capacity retention even after 1000 cycles [110]. In this system, the faradaic lithium-ion intercalation reaction and non-faradaic lithium-ion adsorption/desorption reaction occurred in $LiNi_{0.5}Mn_{1.5}O_4$ and activated carbon, respectively. High energy density and power density asymmetric supercapacitor could be achieved by this new technology of using high potential lithium intercalation compound as the positive electrode and the active carbon as the negative electrode.

7. Conclusions

From this review, it can be suggested that modified high voltage spinel $LiNi_{0.5}Mn_{1.5}O_4$ is one of the promising cathode materials for next generation lithium-ion batteries since they show excellent performances such as good cyclability, rate capability, and thermal stability. Metal dopings on $LiNi_{0.5}Mn_{1.5}O_4$ lead to excellent cycling due to prevention of phase transformation and structural stabilization by dopants. Surface coatings by metal oxides protect the surface of the $LiNi_{0.5}Mn_{1.5}O_4$ by acting like a scavenger of fluoride ions from HF generated from the electrolyte. It is reasonable to suggest that the doping and surface coatings play an important role in improving electrochemical performance of the spinel $LiNi_{0.5}Mn_{1.5}O_4$. Since this spinel cathode material has high nominal voltage of 4.7 V, Ohzuku's group have successfully demonstrated a 3 V lithium-ion cell with $LiNi_{0.5}Mn_{1.5}O_4$ with zero-strain insertion material $Li[Li_{1/3}Ti_{5/3}]O_4$ and the cell showed a quite flat operating voltage of 3.2 V with excellent cyclability [112]. In addition, by selecting the high voltage $LiNi_{0.5}Mn_{1.5}O_4$ material as the positive electrode in combination with an activated carbon negative electrode could provide a new technology to achieve a high energy and power density asymmetric electrochemical supercapacitor.

Acknowledgements

This work is supported by U.S-DOD-ARO-Electrochemistry and Advanced Energy Conversion Division under the grant # W911NF-08-C-0415 (Proposal No: 52322-CH-H (BOBBA)). BRB and R. Santhanam thank Dr. Robert Mantz for supporting cathode materials research for developing hybrid energy storage devices.

References

[1] M.S. Whittingham, Chem. Rev. 104 (2004) 4271.
[2] H.K. Liu, G.X. Wang, Z. Guo, J. Wang, K. Konstantinov, J. Nanosci. Nanotechnol. 6 (2006) 1.
[3] J.M. Tarascon, M. Armond, Nature 414 (2001) 359.
[4] J.W. Fergus, J. Power Sources 195 (2010) 939.
[5] T. Ohzuku, R.J. Brodd, J. Power Sources 174 (2007) 449.
[6] S. Megahed, B. Scrosati, J. Power Sources 51 (1994) 79.
[7] J.M. Tarascon, B. Guyomard, J. Electrochem. Soc. 138 (1991) 2864.
[8] Y. Xia, Y. Zhou, M. Yoshio, J. Electrochem. Soc. 44 (1997) 2493.
[9] B.J. Hwang, R. Santhanam, D.G. Liu, J. Power Sources 101 (2001) 86.
[10] B.J. Hwang, R. Santhanam, C.P. Huang, Y.W. Tsai, J.F. Lee, J. Electrochem. Soc. 149 (2002) A694.
[11] B.J. Hwang, R. Santhanam, D.G. Liu, Y.W. Tsai, J. Power Sources 102 (2001) 326.
[12] B.J. Hwang, R. Santhanam, S.G. Hu, J. Power Sources 108 (2002) 250.
[13] T. Yamada, T. Abe, Y. Iriyama, Z. Ogumi, Electrochem. Commun. 5 (2003) 502.
[14] T. Ohzuku, M. Kitagawa, T. Hirai, J. Electrochem. Soc. 137 (1990) 769.
[15] M.M. Thackeray, Prog. Solid State Chem. 1 (1997) 25.
[16] S. Kobayashi, I.R.M. Kottegoda, Y. Uchimoto, M. Wakihara, J. Mater. Chem. 14 (2004) 1843.
[17] F.K. Shokoohi, J.M. Tarascon, B.J. Wilkens, J. Appl. Phys. 59 (1991) 1260.
[18] K.H. Hwang, S.H. Lee, S.K. Joo, J. Electrochem. Soc. 141 (1994) 3296.
[19] S.H. Park, K.S. Park, Y.K. Sun, K.S. Nahm, J. Electrochem. Soc. 147 (2000) 2116.
[20] A.D. Pasquier, A. Blyr, P. Courjal, D. Larcher, G. Amatuuci, B. Gernand, J.M. Tarascon, J. Electrochem. Soc. 146 (1999) 428.
[21] C. Sigala, D. Guyomard, A. Verbaere, Y. Piffard, M. Tournoux, Solid State Ionics 81 (1995) 167.
[22] K. Amine, H. Tukamoto, H. Yasuda, Y. Fujita, J. Power Sources 68 (1997) 604.
[23] H. Kawai, M. Nagata, H. Kageyama, H. Tukamoto, A.R. West, Electrochim. Acta 45 (1999) 315.
[24] Y.E. Eli, W.F. Howard, S.H. Liu, S. Mukerjee, J. Mcbreen, J.T. Vaughey, M.M. Thackeray, J. Electrochem. Soc. 145 (1998) 1238.
[25] H. Shigemura, H. Sakaebe, H. Kageyama, H. Kobayashi, A.R. West, R. Kanno, S. Morimoto, S. Nasu, M. Tobuchi, J. Electrochem. Soc. 148 (2001) A730.
[26] Q. Zhong, A. Bonakdarpour, M. Zhang, Y. Gao, J.R. Dahn, J. Electrochem. Soc. 144 (1997) 205.
[27] T. Ohzuku, S. Takeda, M. Iwanaga, J. Power Sources 81–82 (1999) 90.
[28] K. Kanamura, W. Hoshikawa, T. Umegaki, J. Electrochem. Soc. 149 (2002) A339.
[29] J.B. Goodenough, in: W. Van Schalkwijk, B. Scrosati (Eds.), Advances in Lithium ion Batteries, Kluwer Academic/Plenum Publishers, 2002, p. 147.
[30] J.H. Kim, S.T. Myung, C.S. Yoon, S.G. Kang, Y.K. Sun, Chem. Mater. 16 (2004) 906.
[31] H. Xia, Y.S. Meng, L. Lu, G. Ceder, J. Electrochem. Soc. 154 (2007) A737.
[32] J. Chen, F. Cheng, Acc. Chem. Res. 42 (2009) 713.
[33] M.G. Kim, J. Cho, Adv. Funct. Mater. 19 (2009) 1497.
[34] D. Jugovic, D. Uskokovic, J. Power Sources 190 (2009) 538.
[35] G. Amatucci, J.M. Tarascon, J. Electrochem. Soc. 149 (2002) K31.
[36] T.F. Yi, Y.R. Zhu, X.D. Zhu, J. Shu, C.B. Yue, A.N. Zhou, Ionics 15 (2009) 779.
[37] B.L. Ellis, K.T. Lee, L.F. Nazar, Chem. Mater. 22 (2010) 691.
[38] Q. Sun, X.H. Li, Z.X. Wang, Y. Ji, Trans. Nonferrous Met. Soc. China 19 (2009) 176.
[39] Z. Chen, H. Zhu, S. Ji, V. Linkov, J. Zhang, W. Zhu, J. Power Sources 189 (2009) 507.
[40] H.S. Fang, Z.X. Wang, X.H. Li, H.J. Guo, W.J. Peng, J. Power Sources 153 (2006) 174.
[41] B.J. Hwang, Y.W. Wu, M. Venkateswarlu, M.Y. Cheng, R. Santhanam, J. Power Sources 193 (2009) 828.
[42] G. Du, Y.N. Li, J. Yang, J. Wang, Mater. Res. Bull. 43 (2008) 3607.
[43] J.F. Yi, C.Y. Li, Y.R. Zhu, J. Sheu, R.S. Zhu, J. Solid State Electrochem. 13 (2009) 913.
[44] X.X. Xu, J. Yang, Y.Q. Wang, Y.N. Nuli, J.L. Wang, J. Power Sources 174 (2007) 1113.
[45] Y.S. Lee, Y.K. Sun, S. Ota, T. Miyashita, M. Yoshio, Electrochem. Commun. 4 (2002) 989.
[46] Y. Fan, J. Wang, X. Ye, J. Zhang, Mater. Chem. Phys. 103 (2007) 19.
[47] Y.K. Sun, S.W. Oh, C.S. Yoon, H.J. Bang, J. Prakash, J. Power Sources 161 (2006) 19.
[48] X. Fang, N. Ding, X.Y. Feng, Y. Lu, C.H. Chen, Electrochim. Acta 54 (2009) 7471.
[49] J.C. Arrebola, A. Caballero, M. Cruz, L. Hernan, J. Morales, E.R. Castellon, Adv. Funct. Mater. 16 (2006) 1904.
[50] H.Y. Xu, S. Xie, N. Ding, B.L. Liu, Y. Shang, C.H. Chen, Electrochim. Acta 51 (2006) 4352.
[51] S.T. Myung, S. Komaba, N. Kumagai, H. Yashiro, H.T. Chung, T.H. Cho, Electrochim. Acta 47 (2002) 2543.
[52] S.H. Oh, S.H. Jeon, W.I. Cho, C.S. Kim, B.W. Cho, J. Alloys Compd. 452 (2008) 389.
[53] W.T. Jeong, K.S. Lee, J. Alloys Compd. 332 (2001) 205.
[54] W.T. Jeong, J.H. Joo, K.S. Lee, J. Alloys Compd. 119–121 (2003) 690.
[55] H. Fang, Z. Wang, B. Zhang, X. Li, G. Li, Electrochem. Commun. 9 (2007) 1077.
[56] F.G.B. Ooms, E.M. Kelder, J. Schoonman, M. Wagemaker, F.M. Mulder, Solid State Ionics 152–153 (2002) 143.
[57] X. Wu, S.B. Kim, J. Power Sources 109 (2002) 53.
[58] X. Yang, W. Tang, H. Kahoh, K. Ooi, J. Mater. Chem. 9 (1999) 2683.
[59] C.H. Han, Y.S. Hong, C.M. Park, K. Kim, J. Power Sources 92 (2001) 95.
[60] W. Tang, H. Kanoh, K. Ooi, J. Solid State Chem. 142 (1999) 19.
[61] L. Wen, Q. Lu, G. Xu, Electrochim. Acta 51 (2006) 4388.
[62] J.H. Kim, S.T. Myung, Y.K. Sun, Electrochim. Acta 49 (2004) 219.
[63] K.S. Martirosyan, D. Luss, J. Alloys Compd. 51 (2005) 2801.
[64] Y.L. Gan, L. Zhang, Y.X. Wen, F. Wang, H.F. Su, Particuology 6 (2008) 81.
[65] L. Zhang, X. Lv, Y. Wen, F. Wang, H. Su, J. Alloys Compd. 480 (2009) 802.
[66] P. Strobel, A.I. Palos, M. Anne, F.L. Cras, J. Mater. Chem. 10 (2000) 429.
[67] H. Kawai, M. Tabuchi, M. Nagata, H. Tukamoto, A.R. West, J. Mater. Chem. 8 (1998) 1273.
[68] K.M. Shaju, P.G. Bruce, Dalton Trans. (2008) 5471.
[69] A. Van der Ven, G. Ceder, Phys. Rev. B 59 (1999) 742.
[70] A. Van der Ven, C. Marianetti, D. Morgan, G. Ceder, Solid State Ionics 135 (2000) 21.
[71] M. Kunduraci, J.F. Al-Sharab, G.G. Amatucci, Chem. Mater. 18 (2006) 3585.
[72] M. Kunduraci, G.G. Amatucci, J. Electrochem. Soc. 153 (2006) A1345.
[73] S. Patoux, L. Sannier, H. Lignier, Y. Reynier, C. Bourbon, S. Jouanneau, F.L. Cras, S. Martinet, Electrochim. Acta 53 (2008) 4137.
[74] J.H. Kim, S.T. Myung, C.S. Yoon, I.-H. Oh, Y.K. Sun, J. Electrochem. Soc. 151 (2004) A1911.
[75] R. Alcantara, M. Jaraba, P. Lavela, J.L. Tirado, Ph. Biensan, A. de Guibert, C. Jordy, J.P. Peres, Chem. Mater. 15 (2003) 2376.
[76] R. Alcantara, M. Jaraba, P. Lavela, J.M. Lloris, C.P. Vicente, J.L. Tiradoz, J. Electrochem. Soc. 152 (2005) A13.
[77] J. Liu, A. Manthiram, J. Phys. Chem. C 113 (2009) 15073.
[78] B. Leon, J.M. Lloris, C.P. Vicente, J.L. Tirado, Electrochem. Solid State Lett. 9 (2006) A96.
[79] M. Aklalouch, J.M. Amarilla, R.M. Rojas, I. Saadoune, J.M. Rojo, J. Power Sources 185 (2008) 501.
[80] S. Rajakumar, R. Thirunakaran, A. Sivashanmugam, S. Gopukumar, J. Electrochem. Soc. 157 (2010) A333.
[81] T.A. Arun Kumar, A. Manthiram, Electrochim. Acta 50 (2005) 5568.
[82] H. Wang, H. Xia, M.O. Lai, L. Lu, Electrochem. Commun. 11 (2009) 1539.
[83] S.H. Oh, K.Y. Chung, S.H. Jeon, C.S. Kim, W.I. Cho, B.W. Cho, J. Alloys Compd. 469 (2009) 244.
[84] C. Locati, U. Lafont, L. Simonin, F. Ooms, E.M. Kelder, J. Power Sources 174 (2007) 847.
[85] X.X. Xu, J. Yang, Y.Q. Wang, Y.N. NuLia, J.L. Wang, J. Power Sources 174 (2007) 1113.
[86] G. Du, Y. Nu Li, J. Yang, J. Wang, Mater. Res. Bull. 43 (2008) 3607.
[87] Y.K. Sun, K.J. Honga, J. Prakash, K. Amine, Electrochem. Commun. 4 (2002) 344.
[88] Y.K. Sun, Y.S. Lee, M. Yoshio, K. Amine, Electrochem. Solid State Lett. 5 (2002) A99.
[89] Y.K. Sun, C.S. Yoon, I.H. Oh, Electrochim. Acta 48 (2003) 503.
[90] Y.K. Sun, Y.S. Lee, M. Yoshio, K. Amine, J. Electrochem. Soc. 150 (2003) L11.
[91] Y. Fan, J. Wang, Z. Tang, W. He, J. Zhang, Electrochim. Acta 52 (2007) 3870.
[92] Y. Kobayashi, H. Miyashiro, K. Takei, H. Shigemura, M. Tabuchi, H. Kageyama, T. Iwahori, J. Electrochem. Soc. 150 (2003) A1577.
[93] R. Alacantara, M. Jaraba, P. Lavela, J.L. Tirado, J. Electroanal. Chem. 566 (2004) 187.
[94] J. Arrebola, A. Caballero, L. Hernán, J. Morales, E.R. Castellon, J.R.R. Barradoc, J. Electrochem. Soc. 154 (2007) A178.
[95] J. Arrebola, A. Caballero, L. Hernan, J. Morales, E.R. Castellon, Electrochem. Solid State Lett. 8 (2005) A303.
[96] H.B. Kang, S.T. Myung, K. Amine, S.M. Leed, Y.K. Sun, J. Power Sources 195 (2010) 2023.
[97] H.M. Wu, I. Belharouak, A. Abouimrane, Y.-K. Sun, K. Amine, J. Power Sources 195 (2010) 2909.
[98] B.E. Conway, Electrochemical Supercapacitors: Scientific Fundamentals and Technological Applications, Kluwer Academic, Publishers, New York, 1999.
[99] K.S. Ryu, Y. Lee, K.S. Han, Y.J. Park, M.G. Kang, N.G. Park, S.H. Chang, Solid State Ionics 175 (2004) 765.
[100] C.C. Hu, T.W. Tsou, J. Power Sources 115 (2003) 179.
[101] J.P. Zheng, T.R. Jow, J. Electrochem. Soc. 142 (1995) L6.
[102] A. Burke, J. Power Sources 91 (2000) 37.
[103] A. Du Pasquier, I. Plitz, S. Menocal, G. Amatucci, J. Power Sources 115 (2003) 171.
[104] W.G. Pell, B.E. Conway, J. Power Sources 136 (2004) 334.
[105] B.H. Huang, P. Yang, B.H. Zhang, Q.M. Shi, J. Power Sources 30 (2006) 560.
[106] F. Chen, R.G. Li, M. Hou, L. Liu, R. Wang, Z.H. Deng, Electrochim. Acta 51 (2005) 61.
[107] A.D. Pasquier, A. Laforgue, P. Simon, J. Power Sources 125 (2004) 95.

[108] Y.G. Wang, J.Y. Lou, W. Wu, C.X. Wang, Y.Y. Xia, J. Electrochem. Soc. 154 (2007) A228.
[109] Y. Zhao, Y.Y. Wang, Q.Y. Lai, L.M. Chen, Y.J. Hao, X.Y. Ji, Synth. Met. 159 (2009) 331.
[110] H. Wu, Ch.V. Rao, B. Rambabu, Mater. Chem. Phys. 116 (2009) 532.
[111] H. Li, L. Cheng, Y. Xia, Electrochem. Solid State Lett. 8 (2005) A433.
[112] K. Ariyoshi, S. Yamamoto, T. Ohzuku, J. Power Sources 119–121 (2003) 959.